A Linear FMCW Radar System for Accurate Indoor Localization and Trajectory Detection

Rongpeng Xiong[1], Xinxin Feng[1], Haifeng Zheng[1] and Zhizhang (David) Chen[2,1]
[1]College of Physics and Information Engineering, Fuzhou University, Fujian, P. R. China
[2]Dept. of Electrical and Computer Engineering, Dalhousie University, Halifax, Nova Scotia, Canada
{N171127042, fxx1116, zhenghf}@fzu.edu.cn; z.chen@dal.ca

***Abstract*—The frequency modulated continuous wave (FMCW) radar has been used to determine the position and movements of a target. In this paper, we design a liner FMCW radar-based indoor position system for better target localization and trajectory detection. First, with the received radar signals, we construct a two-dimensional range-Doppler map. Using the map, We extend the one-dimensional constant-false-alarm rate (CFAR) technique into the two-dimensional one and develop a two-dimensional cell-averaging CFAR detector; it effectively eliminates the outliers of the original CFAR results and hence reduces localization error significantly. Finally, we adopt the Kalman filter to optimize the target trajectory. The experimental results are provided and they show that the accuracy of the estimated range is improved by about 38% and 11% in stationary and moving target localization, respectively, as compared with the current detectors.**

***Index Terms*—Indoor localization, trajectory, frequency-modulated-continuous-wave (FMCW), constant-false-alarm-rate (CFAR), Kalman filter.**

I. Introduction

In recent years, we have witnessed the rapid growth of the Internet of Things (IoT) in both research and applications. It interconnects everything including humans and therefore has attracted extensive attention worldwide. It includes acquisitions, transmission and computing of big data that include localization and tracking movements of a target being goods or humans.

The well-developed global positioning system (GPS) using satellites has been successfully and widely used for outdoor localization and navigation. However, it does not work in indoor settings because of the blockage of the GPS signals by walls and buildings. As a result, other means, especially wireless technologies, have to be utilized and developed.

Ref. [1] presents the comparisons of various indoor wireless localization technologies developed so far and shows that wireless localization technology can be effective, efficient and accurate with easy uses and maintenance. One of them is the radar localization and tracking technologies.

Among the radar technologies, the linear frequency-modulated-continuous wave (FMCW) technology has attracted much attention because it comes with a small blind zone and high precision; the localization accuracy is claimed to reach the micron-scale in [2]. The frequency of the linear FMCW signal increases linearly with time, and the echo signal reflected by a target presents a certain frequency difference from the transmitted signal. Such differences contain the information of the distance, speed, relative position between the target and they can be extracted for tracking the target. Linear FMCW radars have also been used in many extended applications; they include parking monitoring [3], vital sign detection (e.g. heart and respiration rates) [4] [5], heart rate and respiration rate monitoring in [4] and [5], and intrusion detection in [6].

In terms of the LFMCW radar localization techniques, there are various methods, for examples, the methods based on the received signal's time of arrival (ToA) [7] and [8], the received signal's time differences of arrival (TDoA) [9], the received signal strengths indicator (RSSI) method in [10] and the signal's angle of arrival (AoA) [11]. Each of them presents their respective advantages and disadvantages.

In this paper, we develop a localization technique that can determine the range, speed, azimuthal location angle and motion trajectory of a target. In determining the range, we develop a two-dimensional cell averaged CFAR method that can find the indexes associated with the target location from the range-Doppler map through the range bins. In determining the azimuthal angle, we develop and exploit the relationship between the signal's flight distance and phase. In determining the motion trajectory of a target, we connect all the time coordinates and process them. With our method, outliers of the original CFAR results are eliminated and the associated errors are reduced significantly. Besides, we formulate the threshold matrix and reduce the possible background interfering power.

II. The Proposed Method

The linear FMCW radar system under consideration is shown in Fig. 1. The coordinates of the target is denoted as (x, y). Then the location coordinates of the target can be expressed as:

$$\begin{cases} x = R\sin(\theta), \\ y = \sqrt{R^2 - x^2}, \end{cases} \tag{1}$$

where R is the distance or range of the target from the radar and θ is the azimuthal angle at which the target lies at. The receiving antennas are placed at the origin (0,0) (in m).

This work was supported by NSF China (Nos. 61601126, 61571129). Corresponding author: Xinxin Feng.

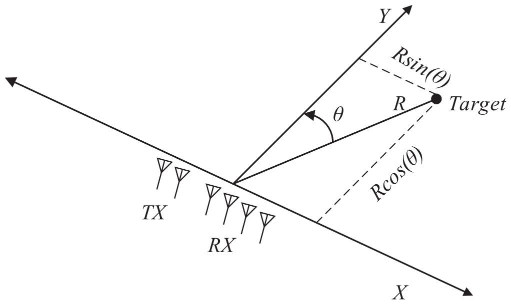

Fig. 1. The line FMCW radar localization system.

A. *Distance (or Range) Measurement*

As mentioned above, the linear FMCW radar emits the repeated linear frequency-modulated continuous-waves, which are also called as chirps. The linear FMCW signals are sent out by the transmitting antennas, incident onto and reflected by the target and then received by the receiving antennas. The received signals are then mixed with the transmitting signals, resulting in an intermediate frequency (IF) signal whose frequency is the frequency difference between the transmitted and the received signals. Suppose that the transmitted signal is $x_1 = sin(\omega_1 t + \varphi_1)$, and the reflected and received signal is $x_2 = sin(\omega_2 t + \varphi_2)$. Then the IF signal is:

$$x_{out} = sin[(\omega_1 - \omega_2) + (\varphi_1 - \varphi_2)] = sin(\omega_{IF} + \varphi_0), \quad (2)$$

where φ_0 is the phase of the IF signal and $\omega_{IF} = 2\pi f_{IF}$ with f_{IF} being the frequency of the IF signal.

Fig. 2 shows the time-frequency of the chirp signals, where the upper diagram shows the transmitted signals and the received (or echo) signals, and the lower diagram shows the IF signals after the mixing. Notice that the received signal is a time delay version of the transmitted signals and the IF signals are valid only in the time interval where both the transmitted signal and the echo signals overlap. The round trip time (RTT) for the signal to travel to the target and back to the receiver is

$$\tau = \frac{2R}{c}, \quad (3)$$

where c is the speed of light and R is the distance of the detected target for the radar.

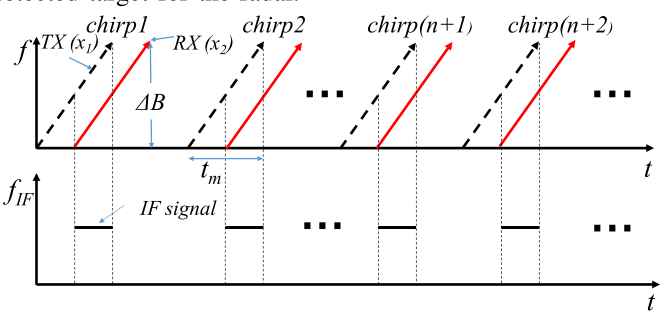

Fig. 2. Signals of the linear FMCW system.

If the continuous transmitted signals have a chirp length t_m and a modulation bandwidth ΔB, the received echo signal reflected from the target is received after an RTT τ. Suppose the the frequency of the IF signal is f_{IF}. By examining Fig. 2, the target distance R is then:

$$R = \frac{c t_m f_{IF}}{2\Delta B}. \quad (4)$$

B. *Angle Detection*

After measuring the distance to the detected target, we need to calculate the azimuthal angle at which the received signals arrive or the target lies, also known as AoA. The enlarged picture at the radar antenna is shown in Fig. 3, where one transmitting antenna and two or more receiving antennas are employed. The AoA is denoted as θ. Considering that the distance to the target is much larger than the space between the two receiving antennas, we can assume that the paths of the echo signals reach the two receiving antennas in parallel. The difference in the signal's travel distances between the two adjacent receiving antennas is

$$\Delta d = l \sin(\theta), \quad (5)$$

where l is the space between two adjacent receiving antennas.

The difference in the signal's travel distance to the receiving antennas lead to the phase differences between the signals received by the receiving antennas. The phase difference is:

$$\Delta\varphi = \omega\frac{\Delta d}{c} = \frac{2\pi\Delta d}{\lambda} = \frac{2\pi l \sin(\theta)}{\lambda}, \quad (6)$$

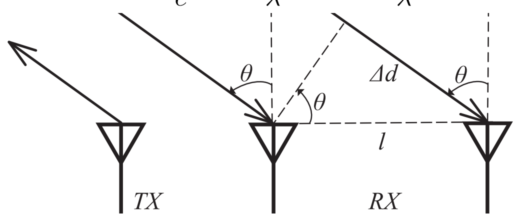

Fig. 3. The AoA estimation.

From (6), the AoA can be obtained as

$$\theta = \sin^{-1}\left(\frac{\lambda\Delta\varphi}{2\pi l}\right), \quad (7)$$

where $\Delta\varphi$ is the phase difference between the received signals of the two adjacent receiving antennas and λ is the wavelength corresponding to the frequency of the transmitted signal.

C. *Signal Processing*

Fig. 4 shows the processing of the IF signal which is converted to the digital data through an ADC. The Fast Fourier Transform (FFT) is applied to the fast-time dimension of data to obtain the range (or distance) and to the slow-time dimension to obtain the Doppler frequency which related to the speed of the target. Note that the IF signals in Fig. 4 is one of the receiving antennas; for the azimuthal angle, signals from at least two receiving antennas are needed.

III. Factors Affecting Localization Results

In real-world measurements, noises and interference always exist and the ADC data collected are contaminated with noises and interference. How to mitigate their influences is a topic of research in the area. In this paper, we quantitatively analyze the impact of these two factors apply optimization to both target detection and coordinate trajectory. We develop the process of Fig. 5 to overcome the problem.

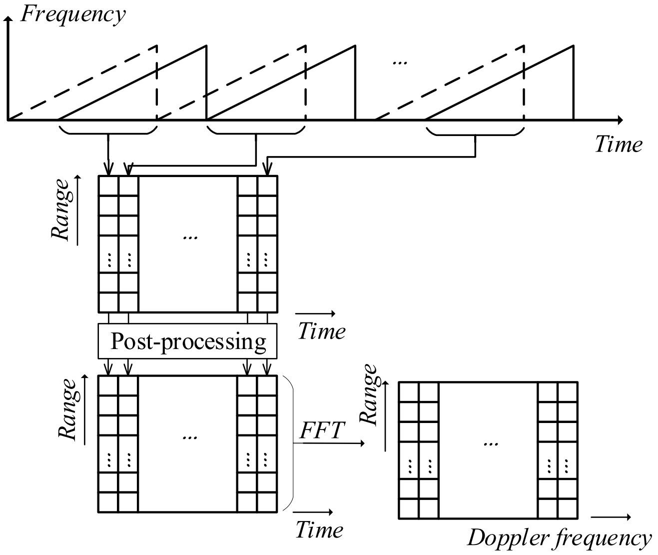

Fig. 4. FFT signal processing diagrams

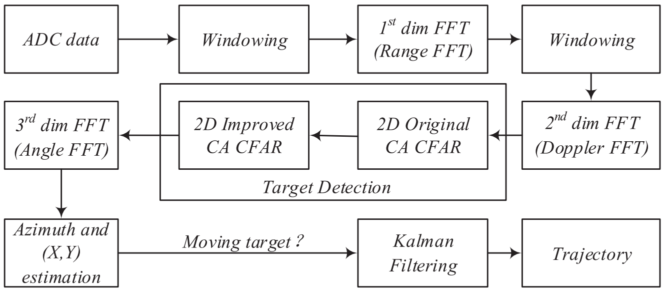

Fig. 5. Block diagram of the ADC data processing process.

A. Target Detection

The purpose of radar target detection is to determine whether the target exists in an FFT results that are contaminated by interference that may come from thermal noise and scatterings from earth, rain, snow, waves, and other clutters. In this paper, the constant-false-alarm-rate (CFAR) detection algorithm is used to detect the target [12] [13]. CFAR is a signal processing algorithm that provides detection thresholds for detection strategies in radar automatic detection systems and minimizes the impacts of interference on the false alarm probability of the system, commonly used in FMCW systems.

In the CFAR detection schemes, we need to set a constant false alarm rate to calculate the power threshold of a specific signal; if the signals are above this threshold, targets are considered to be existent. The threshold values need to be properly set up. If the threshold is too low, the number of false alarms will increase. If the threshold value is too high, the number of false alarms decreases but the number of detected targets decreases too.

The CFAR method we used is called cell-averaging (CA) CFAR, and Fig. 6 shows the processing diagram of the one-dimensional CA CFAR. However, the range-Doppler Map that this experiment needs that is two-dimensional (as shown in Fig. 4). Therefore, we extend the one-dimensional CA CFAR to two-dimensions and propose a more robust and precise target detection method. The flow chart of our purposed method is shown in Fig. 7.

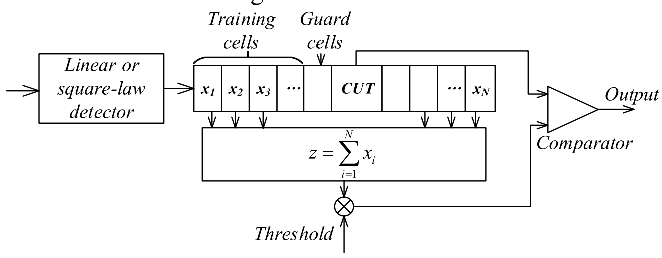

Fig. 6. One-dimensional CA CFAR algorithm.

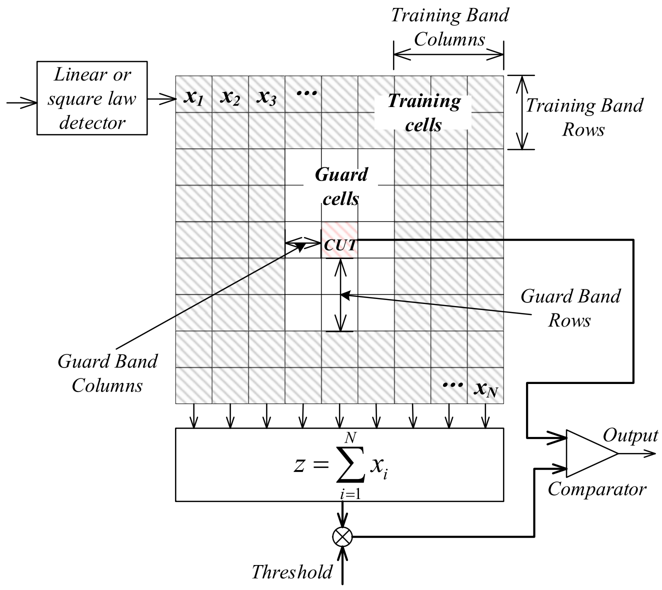

Fig. 7. Two-dimensional CA CFAR algorithm.

In our proposed CA CFAR detection method, we set a block of cells as a training block and estimate the threshold level by their averaged power level. If the total length of the target exceeds the length of one cell, the target corresponding CUT will have a self-masking effect when performing CFAR detection. To avoid using power from the CUT itself that may destroy the estimate, the cells immediately adjacent to the CUT are ignored; these cells are called as “guard cells”.

In our experiments, we assume that noise and background clutter of radar receiver are of independent Gaussian distributions, and the training cells obey the exponential distribution after square law detection. In the homogeneous background, we assume that the training cells samples are statistically independent and have the same distribution; then the probability density function is:

$$p_{x_i}\left(x_i\right) = \frac{1}{\beta^2} e^{-x_i/\beta^2}, \tag{8}$$

where β can estimated with

$$\hat{\beta}^2 = \frac{1}{N} \sum_{i=1}^{N} x_i. \tag{9}$$

As described in the introduction, the presence of interfering targets or clutter edges results in target masking or higher leakage, respectively. To solve these problems, we propose an improved CA CFAR processor, which efficiently solves this problem.

Before performing the improved CA CFAR algorithm, the original two-dimensional CA CFAR needs to be executed first, and the obtained detection result is taken as an input of the improved CA CFAR detector. The algorithm improves the calculation of the threshold. Firstly, the improved background sum after outlier removal is obtained, and then the improved number of cells in training cells is updated. Afterward, the improved multiplication factor is obtained. And finally, the improved threshold is calculated and will be used to detect the Range-Doppler Map to get a new detection result.

B. Trajectory Optimization

A spatial trajectory is a sequence of (x, y) points, each with a timestamp. Since the trajectories are measured by radar, they inevitably have some errors that can be reduced by some forms of data smoothing. In this experiment, we use a Kalman filter [14] which is used to estimate the optimal state of a system.

First, we need to set up proper equations to describe the state of the linear system. Assume that the state equation and the observation equation of the system are:

$$x_k = Ax_{k-1} + Bu_k + w_{k-1}, \tag{10}$$

$$z_k = Hx_k + v_k, \tag{11}$$

where x_k is the state of the system at time k, u_k is the control signal, w_k is the process noise that conforms to the Gaussian distribution and the covariance is Q, z_k is the observation value of the system at time k, and y_k is the measurement noise that conforms to the Gaussian distribution and the covariance is R, A, B, and H are system parameters.

Kalman filtering is an iterative process that at every iteration a new observation is obtained and used to update system state x and error covariance P.

Each iteration is divided into two steps: prediction and correction. In the prediction, the system state and error covariance at the current time are predicted based on the iterative results of the previous moment, namely $\hat{x}_k^-$ and P_k^-:

$$\hat{x}_k^- = A\hat{x}_{k-1} + Bu_k, \tag{12}$$

$$P_k^- = AP_{k-1}A^T + Q. \tag{13}$$

In the correction, the Kalman gain K_k is calculated, along with the actual measurement z_k at the current time. In our case, there is no control signal; therefore, $Bu_k = 0$. Similarly, parameters A and H can be set to 1. They are used to obtain the new $\hat{x}_k$ and P_k as follows:

$$\begin{cases} K_k = \frac{P_k^-}{P_k^- + R}, \\ \hat{x}_k = \hat{x}_{k-1}^- + K_k(z_k - \hat{x}_{k-1}^-), \\ P_k = (1 - K_k)P_k^-. \end{cases} \tag{14}$$

The advantage of Kalman filtering is that it can deal with sensor noise. since the sensors are more or less unreliable. Kalman filtering is a kind of software filter method. The basic idea is that we use the minimum mean square error (MSE) as the best estimation criterion, and adopt the state-space model of signal and noise, using the estimated value of the previous moment and the observation value of the current moment. The estimation of the state variable is updated to obtain the estimated value of the current time, and the algorithm makes an estimate satisfying the minimum mean square error for the signal to be processed according to the established system equation and the observation equation.

IV. Experimental Results

Fig. 8 the prototype of the linear FMCW used for the experiment. It has 4 receiving antennas, 2 transmitting antennas. The frequency range is from 77.18 to 78.72 GHz, which is about 1.54 GHz in bandwidth. The theoretical distance resolution is $\Delta d = c/2B \approx 9.76cm$, where c is the speed of light and B is the bandwidth of the signal. The theoretical angular resolution is about $\Delta\theta = 2/N_v = 0.24rad \approx 14.32°$, where N_v is the number of virtual antennas whose value is the product of the number of transmitting antennas and receiving antennas.

Fig. 8. The liner FMCW radar.

A. Localization of Stationary Targets

First, a localization test is performed on a stationary target. The stationary target is located at coordinates $(0, 1.6)$, $(0, 2.4)$, $(0, 3.2)$, $(0, 4.0)$, $(0, 4.8)$,$(0, 5.6)$ (in m) respectively. The localization results are shown in Fig. 9 in the form of points, the points shown in this figure are the results after averaging the estimated point clouds.

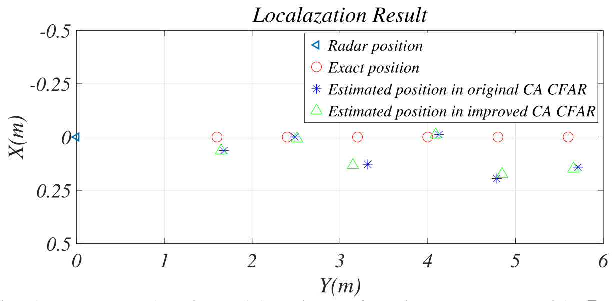

Fig. 9. Exact and estimated locations of stationary targets with $P_{FA} = 5 \times 10^{-8}$.

Table I gives the average localization errors of the original CA CFAR algorithm and our proposed improved CA CFAR algorithm. We calculate the distance between each point in point clouds and the exact point, then calculate the average value of all the obtained distance values as the average range error. It can be seen that the average range error of the improved CA CFAR algorithm is reduced by about 30% compared with the original CA CFAR algorithm; it indicates

TABLE I
AVERAGE RANGE ERROR OF STATIONARY TARGET

Distance	***Original CA CFAR***	***Improved CA CFAR***	***Improvement***
1.6m	0.0812m	0.0485m	40.27$\%$
2.4m	0.0887m	0.0566m	36.19$\%$
3.2m	0.1187m	0.0641m	46.00$\%$
4.0m	0.1298m	0.0924m	28.81$\%$
4.8m	0.1014m	0.0624m	38.46$\%$
5.6m	0.1210m	0.0707m	41.57$\%$

that the improved CA CFAR algorithm is better than the original CA CFAR algorithm in stationary target localization.

B. Tracking of Moving Targets

In the moving target localization, the target moves along the predetermined trajectory. After data collection and processing with the CA CFAR detector, the Kalman filter is applied to obtain the motion trajectory. Fig. 10 shows one of the targets' motion trajectory. The exact trajectory represents the actual movement route, the estimated pointclouds are the points of the moving target and the estimated trajectory is the result after Kalman filtering.

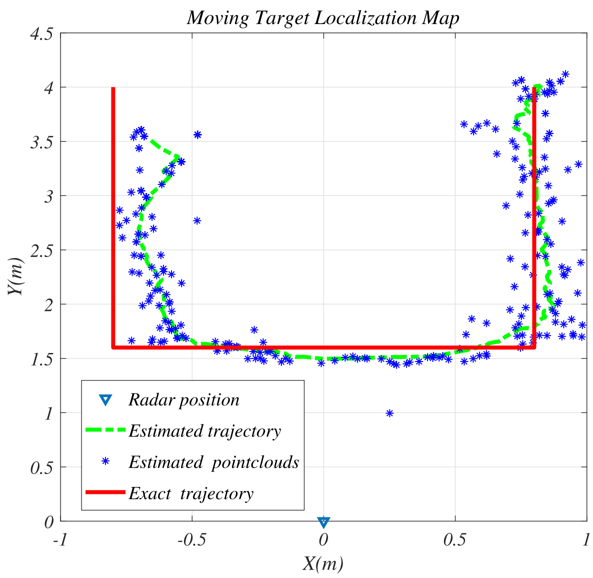

Fig. 10. Estimated trajectory, estimated pointclouds and exact trajectory of a moving target.

The moving target moves at a constant speed in a clockwise direction from the upper right corner. In the process of Kalman filtering, it is also important to choose the appropriate P and Q, which will determine the quality of filtering results. We collected 4 sets of data from moving targets, and the average error of estimated pointclouds and trajectory are shown in **Table II**. This shows that Kalman filtering has played an optimization role, and the average improvement rate in range error is about 11$\%$.

TABLE II
AVERAGE RANGE ERROR OF MOVING TARGET

Sets	***Estimated Point Cloulds***	***Estimated Trajectory***	***Improvement***
1	0.1060m	0.0916m	13.58$\%$
2	0.1142m	0.1032m	9.63$\%$
3	0.1378m	0.1281m	7.04$\%$
4	0.1314m	0.1093m	16.82$\%$

V. CONCLUSION

In this work, we propose a linear FMCW radar-based system to do accurate indoor localization and trajectory reconstruction. The basic principles and implementation methods of Kalman filter and improved CA CFAR are presented. After reasonable parameter selection and setting, pointclouds results are obtained through CA CFAR, and then Kalman filtering is used to further optimize the trajectory of moving targets. Experimental results show that the improved CA CFAR is significantly better than the original method in terms of target detection accuracy. On this basis, the introduction of Kalman filter further improves the accuracy of the target trajectory.

REFERENCES

[1] R. Zekavat and R. M. Buehrer, *Wireless Positioning Systems: Operation, Application, and Comparison*. IEEE, 2019, pp. 3–23. [Online]. Available: https://ieeexplore.ieee.org/document/8633786

[2] M. Pauli, S. Ayhan, S. Scherr, C. Rusch, and T. Zwick, "Range detection with micrometer precision using a high accuracy fmcw radar system," in *International Multi-Conference on Systems, Signals & Devices*. IEEE, 2012, pp. 1–4.

[3] J. M. Garcia, D. Zoeke, and M. Vossiek, "Mimo-fmcw radar-based parking monitoring application with a modified convolutional neural network with spatial priors," *IEEE Access*, vol. 6, pp. 41 391–41 398, 2018.

[4] H. Lee, B.-H. Kim, and J.-G. Yook, "Path loss compensation method for multiple target vital sign detection with 24-ghz fmcw radar," in *2018 IEEE Asia-Pacific Conference on Antennas and Propagation (APCAP)*. IEEE, 2018, pp. 100–101.

[5] M. Alizadeh, G. Shaker, J. C. M. De Almeida, P. P. Morita, and S. Safavi-Naeini, "Remote monitoring of human vital signs using mm-wave fmcw radar," *IEEE Access*, vol. 7, pp. 54 958–54 968, 2019.

[6] T. Kiuru, M. Metso, S. Jardak, P. Pursula, J. Häkli, M. Hirvonen, and R. Sepponen, "Movement and respiration detection using statistical properties of the fmcw radar signal," in *2016 Global Symposium on Millimeter Waves (GSMM) & ESA Workshop on Millimetre-Wave Technology and Applications*. IEEE, 2016, pp. 1–4.

[7] T. Huang, J. Hao, Z. D. Chen, G. Wen, J. Li, and H. Zhao, "An indoor fmcw localization system with the application of the extended kalman filter," in *2018 IEEE MTT-S International Wireless Symposium (IWS)*. IEEE, 2018, pp. 1–4.

[8] B. Al-Qudsi, M. El-Shennawy, N. Joram, and F. Ellinger, "A coverage efficient fmcw positioning system," in *2016 International Conference on Localization and GNSS (ICL-GNSS)*. IEEE, 2016, pp. 1–6.

[9] B. Al-Qudsi, M. El-Shennawy, Y. Wu, N. Joram, and F. Ellinger, "A hybrid tdoa/rssi model for mitigating nlos errors in fmcw based indoor positioning systems," in *2015 11th Conference on Ph. D. Research in Microelectronics and Electronics (PRIME)*. IEEE, 2015, pp. 93–96.

[10] L. Yunxiao and Q. Sujuan, "An improved indoor positioning method based on received signal strengths," in *2015 International Conference on Intelligent Transportation, Big Data and Smart City*. IEEE, 2015, pp. 90–93.

[11] D. Duraj, M. Plotka, M. Rzymowski, K. Nyka, and L. Kulas, "Measurement of distance, velocity and angle of arrival using fmcw-cw combined waveform," in *2016 21st International Conference on Microwave, Radar and Wireless Communications (MIKON)*. IEEE, 2016, pp. 1–4.

[12] J. Guo and Z. D. Chen, "Kurtosis cfar detection for indoor positioning applications with fmcw systems," in *2018 IEEE MTT-S International Wireless Symposium (IWS)*. IEEE, 2018, pp. 1–4.

[13] A. Jalil, H. Yousaf, and M. I. Baig, "Analysis of cfar techniques," in *2016 13th International Bhurban Conference on Applied Sciences and Technology (IBCAST)*. IEEE, 2016, pp. 654–659.

[14] S. G. Mohinder and P. A. Angus, "Kalman filtering: theory and practice using matlab," *John Wileys and Sons*, 2001.